DMD Fast Forward. Published on March 29, 2011 as doi:10.1124/dmd.110.037564

DMD #37564

Metabolism and Pharmacokinetics of Naronapride (ATI-7505), a Serotonin 5-HT_4 Receptor Agonist for Gastrointestinal Motility Disorders

S. Scott Bowersox, Luke K. Lightning, Satish Rao, Monica Palme, Dave Ellis, Renee Coleman, Adrian M Davies, Padmapriya Kumaraswamy, Pascal Druzgala

ARYx Therapeutics, Fremont, CA

Running title: naronapride metabolism and pharmacokinetics

Corresponding author:

S. Scott Bowersox, Ph.D.

ARYx Therapeutics

6300 Dumbarton Circle

Fremont, CA 94555

USA

TEL: 510-585-2200

FAX: 510 585-2201

Email: sbowersox@aryx.com

Number of text pages:

Number of tables: 3

Number of figures: 4

Number of references: 19

Numbers of words in the Abstract: 250

Number of words in the Introduction: 508

Number of words in the Discussion: 1353

Abbreviations: ARC, accurate radioisotope counting; BuChE, butyrylcholinesterase; CYP450, cytochrome P450; HT, hypoxanthine-thymidine; HPLC, high–performance liquid chromatography; KH, Krebs-Henseleit; ATI-7500, 6-[(3*S*,4*R)*-4-(4-amino-5-chloro-2-methoxy-benzoylamino)-3-methoxy-piperidin-1-yl]-hexanoic acid; ATI-7400, 4-[(3*S*,4*R)*-4-(4-amino-5-chloro-2-methoxy- benzoylamino)- 3- methoxy- piperidin- 1-yl]-butanoic acid; ATI-7100, 2-[(3*S*,4*R)*-4-(4-amino-5-chloro-2-methoxy-benzoylamino)-3-methoxy-piperidin-1-yl]-acetic acid;

LC, liquid chromatography; LLOQ, lower limit of quantitation; LSC, liquid scintillation counting; MS, mass spectroscopy; RAD, radio chemical detection

ABSTRACT

The absorption and disposition of the serotonin 5-HT_4 receptor agonist, naronapride (6-[(3*S*,4*R)*-4-(4-amino-5-chloro-2-methoxy-benzoylamino)-3-methoxy-piperidin-1-yl]-hexanoic acid 1-aza-bicyclo[2,2,2]oct-(R)-3-yl ester dihydrochloride), were evaluated in healthy males given a single 120-mg oral dose of ^{14}C-labeled compound. Serial blood samples and complete urine and feces were collected up to 552 hr postdose. Naronapride was extensively metabolized, undergoing rapid hydrolysis to 6-[(3*S*,4*R)*-4-(4-amino-5-chloro-2-methoxy-benzoylamino)-3-methoxy-piperidin-1-yl]-hexanoic acid (ATI-7500) with stoichiometric loss of quinuclidinol. ATI-7500 was either N-glucuronidated on the phenyl ring or its hexanoic acid side chain underwent two-carbon cleavage, probably through a beta-oxidation metabolic pathway, to form 4-[(3*S*,4*R)*-4-(4-amino-5-chloro-2-methoxy- benzoylamino)- 3- methoxy- piperidin- 1-yl]-butanoic acid (ATI-7400). ATI-7400 underwent further side-chain oxidation to form 2-[(3*S*,4*R)*-4-(4-amino-5-chloro-2-methoxy-benzoylamino)-3-methoxy-piperidin-1-yl]-acetic acid (ATI-7100). Quinuclidinol, ATI-7500, ATI-7400, and ATI-7100 were the major metabolites, with plasma AUC values approximately 72-, 17-, 8-, and 2.6-fold that of naronapride. Naronapride, ATI-7500, ATI-7400 and ATI-7100 accounted for 32.32%, 36.56%, 16.28% and 1.58%, respectively, of the dose recovered in urine and feces. ATI-7400 was the most abundant radioactive urinary metabolite (7.77%), and ATI-7500 was the most abundant metabolite in feces (35.62%). Fecal excretion was the major route of elimination. Approximately 32% of the dose was excreted unchanged in feces. Naronapride, ATI-7500, and quinuclidinol reached peak plasma levels within 1 hour postdose. Peak ATI-7400 and ATI-7100 concentrations were reached within 1.7 hour, suggesting rapid ATI-7500 metabolism. Naronapride plasma terminal half-life was 5.36 hr, and half-lives of the major metabolites ranged from 17.69 hr to 33.03 hr. Naronapride plasma protein binding was 30 to 40%. Mean blood-to-plasma radioactivity indicated minimal partitioning of ^{14}C into red blood cells.

INTRODUCTION

Naronapride (6-[(3*S*,4*R)*-4-(4-amino-5-chloro-2-methoxy-benzoylamino)-3-methoxy-piperidin-1-yl]-hexanoic acid 1-aza-bicyclo[2,2,2]oct-(R)-3-yl ester dihydrochloride [ATI-7505]) is an orally-active serotonin 5-HT_4 receptor partial agonist being developed for the treatment of gastrointestinal motility disorders including functional dyspepsia, gastroesophageal reflux disease (GERD), and chronic idiopathic constipation (CIC; Manabe et al., 2010; Camilleri & Bharucha, 2010; Camilleri et al, 2009). Unlike other members of its class (e.g. tegaserod [USFDA Center for Drug Evaluation and Research, 2002; Camilleri, 2001] and cisapride [Mohammad et al, 1997; Pau et al, 2005; Suffredini et al, 2010]), naronapride has relevant affinity for only the 5-HT_4 receptor subtype (K_i = 1.4 nM), negligible affinity for K_v11.1 channels (hERG; K_i = 24,500 nM; Palme et al, 2004) and no effect on cardiac repolarization (Palme et al, 2005; Milner et al., 2010). When tested in wide-spectrum *in vitro* screening assays using radioligand binding techniques, naronapride (≥10 µM) was found to significantly interact with several binding sites in addition to the 5-HT_4 receptor; however, taking expected therapeutic plasma concentrations into account, only an interaction with the dopamine D_2 receptor (Ki = 61 nM for D_{2L}) appears to have the potential to be clinically relevant. Dose-related increases in prolactin levels noted in rats after single dose administration of naronapride suggest D_2 receptor antagonism (unpublished observations). Prolactin elevation has not been observed in humans at clinically effective doses. (ARYx Therapeutics, unpublished observations).

Although the clinical implications of this interaction are not known at this time, observed dose-related increases in prolactin levels noted in rats after single dose administration of naronapride suggest a relationship to D_2 receptor antagonism (unpublished observations).

Like other high-affinity 5-HT_4 receptor agonists (e.g. cisapride, tegaserod, prucalopride), naronapride is a potent enterokinetic agent and, in animal models, has been shown to increase upper and lower-bowel motility when it is administered orally, systemically, or intracolonically (ARYX Therapeutics, unpublished findings; Balemba & Mawe, 2009). Results of clinical studies

carried out to date indicate that oral naronapride increases gastric and colonic motility in healthy volunteers (Camilleri et al., 2007), decreases gastric acid exposure to the esophagus and increases symptom-free days of nocturnal heartburn and dyspeptic symptoms in patients with symptomatic GERD (ARYx Therapeutics, unpublished results). In a recent Phase 2 study in CIC patients, naronapride increased spontaneous bowel movements and decreased the time to first bowel movement (Palme et al., 2010). Naronapride is currently in late-stage clinical development for the treatment of CIC.

The objective of this investigation was to determine the absorption, metabolism, and excretion of naronapride in healthy male subjects given a single oral dose of ^{14}C-labeled compound (Fig 1). To elucidate metabolic and excretory pathways, major and minor metabolites were identified and quantified in plasma, urine, and feces. The pharmacokinetics of naronapride and its metabolites after a single oral naronapride dose were also determined. To investigate the role of CYP450 monooxygenases in naronapride biotransformation, the metabolic profile of naronapride in human liver microsomes was determined in the presence and absence of an nicotinamide adenine dinucleotide phosphate (NADPH)-generating system. The metabolic profile of naronapride was also determined using cryopreserved human hepatocytes to assess Phase I and Phase II metabolic activity.

METHODS

Clinical Study Design. After an overnight fast, 8 healthy male volunteers received a single 120 mg (approximately 200 µCi) oral dose of [^{14}C]-naronapride in a liquid formulation. Dose selection was based on the outcomes of a previous single and multiple ascending oral dose study in healthy volunteers; 120 mg is in the upper range of potential clinical doses. In a multiple ascending dose study, single doses of 120 mg resulted in detectable plasma concentrations of naronapride persisting to approximately 72 hrs postdose, providing a sufficient length of time to determine its metabolic fate. Tissue and whole-body exposure to radioactivity

was expected to be minimal (i.e. less than 5% of the allowable amount) at this dose based on the dosimetry analysis of the results from a quantitative whole-body autoradiography tissue distribution study in rats. Biological samples were collected for up to 552 hrs after dosing. Blood and plasma were collected predose, 0.5, 1, 2, 3, 4, 6, 8, 12, 16, 20, 24, 36, 48, 72, 96, 120, and 144 hrs postdose into vacutainers containing 1% ethanolic paraoxon to prevent *ex vivo* hydrolysis. Urine was collected predose, and 0-2, 2-4, 4-8, 8-12, 12-24, 24-36, 36-48 hrs postdose and at 24 hr intervals thereafter, as applicable. Feces was collected predose and at 24 hr intervals as applicable. Blood, collection and/or analysis of samples was discontinued when the concentration of radioactivity in blood, plasma, urine, and feces were equal to or less than 2-times the matrix background activity or after ≥90% of the dose radioactivity was recovered in urine and feces. Samples were analyzed for total ^{14}C radioactivity. Metabolite identification and profiling was accomplished using HPLC/MS/RAD methods. Naronapride and its major metabolites were measured in selected plasma samples using LC/MS. Pharmacokinetic analyses of the individual blood and plasma radioactivity and plasma concentrations of naronapride and its major metabolites were conducted using a non-compartmental approach with the validated computer program WinNonlin (ver. 5.1.1). For blood and plasma radioactivity, the pharmacokinetic parameters determined included C_{max}, t_{max}, AUC and blood to plasma radioactivity AUC ratio. For plasma naronapride and its major metabolites, the pharmacokinetic parameters determined were C_{max}, t_{max}, AUC_{∞}, $t_{1/2,z}$, Cl_o, CL_r, V_z/F and metabolic AUC ratios. For urine and feces radioactivity, including naronapride and major metabolites, the pharmacokinetic parameters were the cumulative recovery of radioactivity and analytes.

This study was performed in accordance with local regulations and the principles of the Declaration of Helsinki, its amendments (6^{th} Revision, 59^{th} WMA General Assembly, Seoul, October 2008) and Good Clinical Practice.

Test Article and Dose Formulation. Test articles and standards (naronapride, ATI-7500, ATI-7400, AT-7100, quinuclidinol, naronapride-d3, ATI-7500-d3, ATI-7400-d3, ATI-7100-d3) were provided by either ARYx Therapeutics (Fremont, CA) or Procter & Gamble Pharmaceuticals Process Development (Norwich, NY). Naronapride (radiochemical purity 99.15%) and [^{14}C]-ATI-7500 (radiochemical purity 97.4%) prepared by Ricerca Biosciences (Concord, OH) was used for *in vitro* plasma protein studies. A mixture of [^{14}C]-naronapride (radiochemical purity 98.9%) and naronapride manufactured by Ricerca Biosciences (Concord, Ohio) was used for dosing. The dose was administered in 20 mL of Ora-Sweet solution (Ora-Sweet and sterile water). The dosing container was rinsed twice with portions of 240 mL of distilled water after dose administration; the rinse portions and all of the remaining water was also ingested by the subject.

All dose formulations were analyzed for radioactivity concentration by liquid scintillation counting (LSC) [Model 2900TR, Packard Instrument Company] and specific activity. After dose administration, the empty treatment bottle for each subject was analyzed by adding a weighed amount of ethanol:H_2O (20:80, v:v) to each bottle and analyzing duplicate weighed samples of each extract by LSC. Residual radioactivity recovered from each treatment bottle was subtracted from the dose administered to the respective subject. All dose formulations were stored at approximately -20°C before and after analysis. All personnel followed standard safety precautions as required by laboratory policies and procedures in consideration of Material Safety Data Sheets and other relevant safety information.

HPLC Radio-analysis and HPLC/MS System. Naronapride and its metabolites were separated using reverse phase liquid chromatography and detected by a radio flow-through detector and linear trap quadrupole mass spectrometer simultaneously. The system for metabolite profiling and identification consisted of a Finnigan autosampler, a Surveyor HPLC pump, an LTQ mass spectrometer, and a β-RAM Model 3 radio flow-through detector (Perkin Elmer, Waltham, MA). The mass spectrometer was controlled by Xcalibur (ThermoFisher

Scientific, Pittsburg, PA) software, and the radio flow-through detector was controlled by Laura Lite 3 (LabLogic Systems, Brandon, FL). The HPLC eluent was split between the radio flow-through detector and MS with a ratio of 3 to 1. HPLC separation was carried out using a Phenomenex Synergi Max RP, 250 X 4.6 mm, 5 µm column. The mobile phase was A: 0.1% formic acid in 5 mM ammonium formate, B: 0.1% formic acid in MeOH; %B was cycled from 10% to 90% to 10% over 35 minutes at a flow rate of 800 µL/minute. Mass spectrometry conditions were as follows: sheath gas: 50 unit, auxiliary gas: 20 unit, sweep gas: 10 unit, ion spray voltage: 5 kV; capillary temperature: 350°C, capillary voltage: 47 V, tube lens voltage: 100 V, and the ionization mode: ESI+.

Two systems were used for radio-quantification. One was an HPLC/Accurate Radioisotope Counting (ARC) system which consisted of a HTC PAL autosampler, two Shimadzu HPLC pumps, a β-RAM Model 3 radio flow-through detector, and a dynamic flow controller. The system was controlled by ARC Data System. The HPLC conditions for this system were the same as the first HPLC/MS. The cell volume for the radio flow-through detector was 800 µL, and all HPLC eluent went through the detector. Another system was an HPL/TopCount™ system which consisted of a HTC Pal autosampler, two Shimadzu HPLC pumps, and a Foxy Jr. Fraction Collector (Isco, Lincoln, NE). HPLC fractions collected in a LumaPlate™ 96-well plate were dried using an EZ-2^{plus} Personal Evaporator (Genevac, Valley Cottage, NY), and the dried samples were counted by TopCount™ NXT Microplate Scintillation & Luminescence Counter (PerkinElmer, Waltham, MA). The data were processed using ProFSA (PerkinElmer, Waltham, MA) software.

Radio-analysis. The HPLC/ARC system was used for radio-quantification of all urine and fecal samples and of plasma samples with radioactivity exceeding 500 dpm/mL. HPLC fraction collection followed by counting with TopCount™ was used for radio-quantification of plasma samples with radioactivity between 200-500 dpm/mL.

All samples were stored at -70°C before analysis. Bulk fecal samples were stored at approximately -20°C after analysis. Duplicate blood (0.2 mL), urine (0.2 g), and fecal samples (approximately 0.5 gm) were combusted (Model 307 Sample Oxidizer, Packard Instrument Company) then analyzed by LSC. Fecal samples were prepared for analysis as follows: Samples from each subject collected during a given 24 hr collection interval were pooled and then weighed. Each was mixed with a weighed amount of 20% aqueous ethanol to create a slurry spiked with a 1% paraoxon solution in ethanol (5 µL/g of feces) to prevent hydrolysis during processing, homogenized using a probe-type homogenizer, and then weighed. Two subsamples (approximately 25 g each) were transferred to labeled containers for metabolite profiling. In addition, a 10 g subsample was taken for supplementary metabolism analysis. After combusting the samples, the resulting $^{14}CO_2$ was trapped in a mixture of Permafluor® and Carbo-Sorb®. Oxidation efficiency was evaluated on each day of sample combustion by analyzing a commercial radiolabeled standard, both directly in scintillation cocktail and by oxidation. Results were compared, and results were accepted if combustion recoveries ranged from 95 to 105%. Ultima Gold XR™ scintillation cocktail was used for samples analyzed directly. All samples were analyzed for radioactivity by LSC for at least 5 minutes or until 100,000 counts were recorded (Model 2900TR liquid scintillation counter, Packard Instrument Company, Meridien, CT). Sample size permitting, all samples were analyzed in duplicate. If results from sample duplicates (calculated as ^{14}C dpm/g sample) differed by more than 10% from the mean value, the sample was homogenized again and then reanalyzed (sample size permitting). This specification was met for all sample aliquots that had radioactivity greater than 100 dpm. Scintillation counting data were automatically corrected for counting efficiency using the external standardization technique and an instrument-stored quench curve generated from a series of sealed quenched standards.

Extraction Recovery of Fecal Samples. Extraction recovery of fecal samples was determined in 24 hr and 72 hr fecal homogenate samples (approximately 2 g each) from one subject.

Samples were thawed, and triplicate aliquots (approximately 0.4 g each) were combusted. The combustion products were mixed with 10 mL of Carbosorb® and 10 mL of Permafluor® before counting using LSC. The radioactivity in the fecal homogenate was defined as 100%. Approximately 2 g aliquots from the 24-hr and 72-hr samples were thawed and extracted with three volumes of methanol/acetonitrile/formic acid (25:75:0.5, v:v:v). Each mixture was vortexed for 3 minutes, sonicated for 5 minutes, and centrifuged at 3000 rpm for 5 minutes. The supernatant was transferred to a clean tube, and the pellet was re-extracted two more times using 3 volumes of the MeOH:ACN:formic acid mixture. The radioactivity of the combined supernatant was determined by LSC, and the extraction recovery was calculated.

Extraction for Metabolite Identification and Profiling. Plasma, urine, and fecal samples were collected at multiple time points before and after [^{14}C]-naronapride dosing. All samples were stored at -70°C until analyzed. To ensure accurate radio-quantitation, samples with greater than 200 dpm/mL for plasma, 1000 dpm/mL for urine, and 2000 dpm/mL for fecal homogenate were used for quantitative analyses and metabolite identification. Plasma samples taken at 0.5, 1, 2, 4, and 8 hrs post-dose, all urine samples of all collection intervals out to 160 hr postdose, and all fecal samples collected at 24 hr intervals beginning 24 hrs postdose and ending 360 hrs postdose were processed for analysis.

Plasma samples from individual subjects were extracted by protein precipitation with acetonitrile and methanol. Plasma samples from each subject at each time point were aliquoted in triplicate (~1.0 mL aliquots), and 1.0 mL of 25% MeOH in H_2O were added to each. After gentle mixing, three volumes (3.0 mL) of acetonitrile were added, vortex-mixed at a low speed and then centrifuged at 500 rpm for approximately 3 minutes. The supernatant was removed and placed in a clean, pre-weighed tube. Pellets were resuspended in 25% MeOH in H_2O and re-extracted by addition of acetonitrile, followed by centrifugation. The supernatants were combined, dried down with a nitrogen stream and reconstituted using 1.0 mL of 100% MeOH. The tubes were rinsed with the reconstitution solvent and were carefully pooled into one tube,

dried down, and then reconstituted using 10% MeOH containing 1% formic acid. The final product was transferred to micro-centrifuge tubes and centrifuged at 15,000 rpm for 45 minutes to separate any residue, counted for radioactivity using LSC for extraction recovery and used for analysis. Each sample represented at least 85% of the total radioactivity for that sample.

Urine samples were centrifuged at 3000 rpm for 5 minutes, and the supernatant was used for analysis.

Fecal homogenate samples with radioactivity greater than 2000 dpm/gm from all subjects (approximately 5 g each) were extracted following the method used to determine extraction recovery as described above. For fecal samples with more than 10,000 dpm/mL, 2 g of sample were used. The supernatants from the extraction of each sample were evaporated to dryness in a 20°C H_2O bath under a stream of nitrogen. Residues from each sample were reconstituted in 1.0 mL of a reconstitution solvent consisting of 99% MeOH and 1% formic acid. The reconstituted samples were again evaporated to dryness under a stream of nitrogen and reconstituted in 1.0 mL MeOH:H_2O:formic acid (10:90:1, v:v:v). The supernatants were then transferred to vials with glass inserts for analysis.

Urine and Feces HPLC Column Recovery. Samples (200 µL) were injected onto the HPLC system, and the eluent from 0 to 27 minutes was collected into a clean 50 mL centrifuge tube. The total volume of eluant was recorded after collection. Triplicate aliquots (200 µL) of the HPLC eluant were counted using an LSC (Tri-Carb 2800TR, PerkinElmer, Waltham, MA). The average value of counting results was used to calculate the total radioactivity contained in the first collected eluant. Another 200 µL sample from the same subject and time point was injected into an HPLC system without the column installed, and the eluant from 0 to 10 minutes was collected into another clean 50 mL centrifuge tube. The total volume of eluant was recorded after collection. Triplicate aliquots (200 µL) of the HPLC eluant were counted using the LSC. The average value of counting results was used to calculate the total radioactivity contained in the second collected eluant.

Analysis and Metabolite Identification. HPLC/tandem mass spectroscopy coupled with radio flow-through detection was used for metabolite profiling and identification. The retention times of the metabolites were determined by the peaks on radio-chromatograms, and the molecular ions of the metabolites were determined on the full scan mass spectra corresponding to the retention times of metabolites on the radio-chromatograms. Tandem MS of the molecular ions was performed, and the structures of the metabolites were assigned based on interpretation of their mass spectra. The molecular weights of the major metabolites (representing ≥5% of the total radioactivity in a matrix compartment) were determined using LC/MS with various ionization modes and searching techniques (precursor ion scan and neutral loss scan). Metabolite structures were confirmed using authentic standards of naronapride, ATI-7500, ATI-7400 and ATI-7100 (ARYx Therapeutics, Fremont, CA).

Quantification of Naronapride and Metabolites. Quantification of naronapride and its metabolites at each collection period was based on the integration of peaks on their radio-chromatograms. For plasma samples, the percent of total radioactivity in the sample for each peak at each time point was calculated, and was converted to ng equivalent (ng-Eq) of parent/mL. For urine and fecal samples, the percent of total radioactivity in the sample for each peak at each time period was calculated and was compared to ng-Eq of parent/g and to the percent of the administered dose. The limit of quantification for radioactivity was defined as the ratio of signal to noise (3:1) on the radiochromatogram. The limit of quantification was 100 dpm for the HPLC/ARC system and 12 dpm for TopCount™.

Due to the low radioactivity detected in the plasma samples and to provide better characterization of metabolite concentration-time profiles, LC/MS methods were developed and used for the measurement of naronapride and its major metabolites in addition to the simultaneous radio flow-through detection and mass spectroscopy method. The analysis was by gradient HPLC using either a Phenomenex Synergi Max RP 100A, 50 x 2 mm (for naronapride, ATI-7500, ATI-7400, and ATI-7100), 2.5 µm or Atlantis HILIC Silica, 30 x 2mm, 5

µm column (for quinuclidinol). The mobile phase was A: 0.1% formic acid in 5 mM ammonium acetate, B: 0.1% formic acid in 90/10 acetonitrile/50 mM ammonium acetate (for naronapride and ATI-7500) or 0.1% formic acid in 100% MeOH (for ATI-7400 and ATI-7100) at flow rates of either 350 µL/min (naronapride and ATI-7500) or 300 µL/min (ATI-7400 and ATI-7100). The mobile phase for determination of quinuclidinol was A: 0.1% formic acid in 10 mM ammonium formate, B: 0.1% formic acid in 97.5/2.5 acetonitrile/10 mM ammonium formate at a flow rate of 300 µL/min. Authentic quinuclidinol, naronapride, ATI-7500, ATI-7400, and ATI-7100 were reference standards and deuterated naronapride, ATI-7500-d3, ATI-7400-d3, and ATI-7100-d3 were internal standards. Samples were analyzed on a Sciex API 5000 (Applied Biosystems) triple quadrupole mass spectrometer equipped with an ESI source. The electrospray interface was operated at 4.5 kV, and the mass spectrometer was operated under multiple reaction monitoring conditions in the positive ion mode. Monitoring transitions for naronapride, ATI-7500, ATI-7400, ATI-7100, and quinuclidinol were (*m/z*) 537.3→184, 428.2 →184, 400.2→184, 372.2→184, and 128.1→110, respectively. The limits of detection were 0.1 ng/mL (naronapride, ATI-7500, ATI-7400, ATI-7100) and 5 ng/mL (quinuclidinol)

***In Vitro* Metabolism: Hepatic Microsomes.** InvitroGRO HT medium, InvitroKHB buffer, and InVitro CP buffer were obtained from Celsis (Chicago, IL). Pooled human liver microsomes from 50 male and female donors were obtained from Xenotech, (Lenexa, KS). Trizma $MgCl_2$, glucose-6-phosphate, glucose-6-phosphate dehydrogenase, and β-$NADP^+$, were obtained from Sigma-Aldrich (St. Louis, MO). DMSO and acetonitrile were obtained from EMD Scientific (Gibbstown, NJ). Methanol, formic acid, and H_2O (HPLC grade) were obtained from Fisher Scientific (Pittsburgh, PA) and 48-well collagen coated plates were obtained from Becton Dickinson (Bedford, MA).

Naronapride (ARYx Therapeutics, Fremont, CA) was prepared at 20 mM in DMSO, diluted to 0.2 mM in acetonitrile/H_2O (80:20), then incubated (37^{o}C) at a final concentration of 2

μM in a Tris buffer (50 mM containing 5 mM $MgCl_2.6H_2O$, pH 7.4) with microsomes (1 mg/mL protein). Incubations were carried out in the presence and absence of an NADPH regeneration system ($NADP^+$, 0.125 mg/mL, glucose-6-phosphate, 0.5 mg/mL, and glucose-6-phosphate dehydrogenase, 0.38 units/mL). Additional incubations were carried out in the absence of microsomes. At various time points (0, 5, 15, 30, 60, 90 minutes), a 50 μL aliquot was removed and added to 100 μL acetonitrile containing an internal standard (0.1 μM ATI-7500-d3 in acetonitrile or 100 μL of ATI-20019 at 0.5 μg/mL). The internal standards were provided by ARYx Therapeutics (Fremont, CA). The samples were centrifuged at 14,000 rpm for 15 minutes at 4^oC, and the supernatant was subject to analysis by HPLC/MS/MS. The analysis was by gradient HPLC using an Agilent Eclipse XDB-C18, 100 x 2.1 mm, 3.5 μm column. The mobile phase was A: 0.1 % formic acid in HPLC H_2O, B: 0.1 % formic acid in acetonitrile at a flow rate: 0.2 mL/min. The conditions were 35% B rising to 95% B over 4 minutes and held for 1 minute then 35% B held for 1 minute. The metabolites were detected using a Sciex API 3000, API 3200, or API 4000 HPLC/MS/MS system with Analyst 1.4.1 Operating and Quantitation software (Concord, ON).

***In Vitro* Metabolism: Hepatocytes.** Plateable cryopreserved human hepatocytes obtained from Celsis (Chicago, IL) were rapidly warmed in H_2O at 37^oC. When almost thawed, they were transferred to a 50 mL conical tube containing 40 mL of pre-warmed HT medium. The hepatocytes were then centrifuged at 2000 rpm for 10 min, and the HT medium was removed. The pellet was resuspended in Krebs-Henseleit (KH) buffer (10 mL), and the viability of the cells was determined by the Trypan blue method. Cells were only used if the viability exceeded 75%. Cell suspensions were aliquoted (594 μL) into 15 wells of a 24-well plate. An equal volume of KH buffer was aliquoted into 5 wells to serve as controls.

Incubations were initiated by addition of non-radiolabeled naronapride at a final concentration of 10 μM. Diclofenac (100 μM, Sigma-Aldrich, St. Louis, MS) was included and

diclofenac hydroxylation and glucuronidation was monitored in all preparations as positive controls to insure that Phase I and Phase II enzymes were active. A separate set of control incubations were performed to determine the stability of the test articles in KH buffer. The plates were incubated at 37^{o}C with 5% CO_2. Aliquots (50 µL) were removed from each well at 0, 0.5, 1, 2, 4 and 6 hr after the addition of the test articles. These were added to 100 µL of acetonitrile (with 0.1% formic acid and internal standard). ATI-7500-d3 was used as the internal standard for naronapride and the ATI compounds. Dextrorphan (Sigma-Aldrich, St. Louis, MS) was used as the internal standard for the diclofenac samples. All samples were thoroughly mixed and subjected to one freeze-thaw cycle on dry ice, then centrifuged at 14,000 rpm for 15 minutes at 4^{o}C to pellet the protein then transferred to HPLC vials and injected into an LC/MS/MS for analysis of naronapride, ATI-7400, and ATI-7100. For the analysis of ATI-7500 and diclofenac, the supernatant was further diluted with H_2O. Calibration standards were prepared separately for each of the test articles.

The analysis was by gradient HPLC using a Phenomenex Synergi Polar-RP, 75 x 3 mm, 4 µm column. The mobile phase was A: 0.1 % formic acid in HPLC H_2O, B: 0.1 % formic acid in acetonitrile at a flow rate: 0.3 mL/min. Gradient conditions for naronapride and its metabolites were: 10% B rising to 95% B over 3 minutes and held for one minute, then declining to 10% B over 1 minute and held for 1 minute. Gradient conditions for diclofenac were: 40% B rising to 90% B over 5 minutes and held for 1 minute, then 40% B held for 2 minutes. The metabolites were detected using a Sciex API 3200 QTrap LC/MS/MS system with Analyst 1.4.2 Operating and Quantitation software (Concord, ON).

***In Vitro* Plasma Protein Binding.** The binding of [^{14}C]-naronapride and its primary metabolite, [^{14}C]-ATI-7500, to plasma proteins was determined by equilibrium dialysis against a Tris buffer (25 mM containing 0.15 M NaCl adjusted to pH 7.4 with 0.1 N hydrochloric acid or 0.1 N sodium hydroxide) using Rapid Equilibrium Dialysis (RED) devices (Thermo Scientific, Rockford, IL). Compounds were prepared in 50% ethanol at convenient concentrations for achieving the

desired assay conditions, with serial dilutions used across each single species. The amount of ethanol in the plasma samples increased from 0.015 to 1.5% in direct proportion to the analyte levels. The presence of ethanol in plasma samples did not change the plasma protein binding of [^{14}C]-naronapride or [^{14}C]-ATI-7500. All measurements were made in triplicate. To inhibit *in vitro* hydrolysis of [^{14}C]-naronapride by plasma esterases, paraoxon was added at a concentration of approximately 40 µg/mL to all plasma samples containing [^{14}C]-naronapride. The presence of paraoxon did not appreciably affect the [^{14}C]-naronapride plasma protein binding values, as the values were unchanged when the amount of inhibitor was increased from 40 to 80 µg/mL. Plasma samples were incubated at 37°C and oscillated at 100 RPM for 9 hours. Using HPLC separation and flow-through radioactivity detection, [^{14}C]-naronapride and [^{14}C]-ATI-7500 were found to be stable at 37°C in plasma and buffer over this period. Plasma protein binding was determined at 0.045, 0.45, 4.5, 45 and 450 µM for [^{14}C]-naronapride and 0.064, 0.64, 6.4, 64, and 640 µM for [^{14}C]-ATI-7500 using liquid scintillation counting (Liquid Scintillation Analyzer, Packard 2550 TR/LL, Waltham, MA). Test article concentrations were chosen to give counts of radioactivity that were distinguishable from background and at least 10-fold higher than expected peak plasma concentrations *in vivo*. The unbound fraction, corrected for the potential presence of a volume shift, was calculated after the manner of Boudinot & Jusko (1984).

Plasma protein binding of the naronapride metabolites, ATI-7400 and ATI-7100, was determined by centrifigation/ultrafiltration using non-radiolabeled standards (ARYx Therapeutics, Fremont, CA). Human plasma was spiked with stock solutions of the test articles prepared in DMSO to yield final concentrations of 2.5 µM and 10 µM. The spiked samples were pH-adjusted to 7.4, if necessary, using dilute HCl, incubated at 37°C at 300 rpm (Eppendorf Thermomixer) for 1 hour and then transferred to ultracentrifugation devices (Centrifree YM-30, Millipore Corp, Bedford, MA) and centrifuged at 1450 x g for 30 minutes. The resulting ultrafiltrate samples were frozen at -70°C until analysis. For sample analysis, 25 µL of the

ultrafiltrate samples and calibration standards were pipetted into a deep-well 96-well plate. To this were added 50 µL of 0.1% formic acid in acetonitrile containing internal standards (ATI-7100-d3 for ATI-7100 and ATI-7400-d3 for ATI-7400 both at 500 ng/mL; deuterated samples supplied by ARYx Therapeutics, Fremont, CA) and 125 µL of 0.1 % formic acid in HPLC H_2O. Samples were mixed well and then centrifuged at 3700 rpm in an Eppendorf 5804R centrifuge for 15 minutes. Chromatographic separation of supernatant samples (10 µL) was achieved using an Agilent Eclipse XDB-C18 column (100 x 2.1 mm, 3.5 µ). The mobile phase was A: water containing 0.1% formic acid, B: acetonitrile containing 0.1% formic acid at a flow rate of 0.2 mL/min. The gradient elution program (%B) was 0.0→1.5 min (30%), 1.5→ 2.00 min (95%), 2.00→3.00 min (30%). Analytes were measured using a TurbolonSpray Sciex API 4000 MS/MS system operated in multiple reaction monitoring mode with positive electrospray ionization and Analyst 1.4.2 software. Multiple reaction monitoring transitions for the test articles and the internal standards were *m/z* 400.1→184.30 (ATI-7400), 372.02→184.10 (ATI-7100), 403.15→187.10 (ATI-7400-d3), 374.84→187.2 (ATI-7100-d3). Peak area ratios of analytes to internal standards were calculated for duplicate standard curves in the range of 5 – 20,000 nM.

Data Analysis. Statistical analyses were limited to simple expressions of variation, such a mean and standard deviation.

RESULTS

Dose Administration. The mean concentration of radioactivity in the subject dose formulation was 2.01 x 10^7 dpm/g. This value and the specific activity determined in a mock dose analysis (1.76 µCi/mg) were used to determine the amount of dose administered to each subject and in the study calculations. Doses ranged from 115 mg to 116 mg/subject (204 to 205 µCi/subject) and were close to the target dose of 120 mg (200 µCi).

Radio-analysis. Concentrations of radioactivity in blood and plasma are presented graphically in Figure 2. The maximum mean concentrations of drug-derived radioactivity in blood and plasma were observed at approximately 1 hour post-dose, with values of 153 and 232 ng-Eq/mL, respectively. Maximum blood radioactivity concentrations in individual subjects were observed from 0.5 to 1 hour postdose and ranged from 81.0 to 319 ng-Eq/mL. Maximum plasma radioactivity concentrations in individual subjects were also observed from 0.5 to 1 hour post-dose and ranged from 124 to 507 ng-Eq/mL. Levels of radioactivity fell below the limit of quantitation in all subjects by 6 and 12 hours post-dose in blood and plasma, respectively. Mean blood:plasma concentration ratios ranged from 0.570 to 0.683 through 4 hours post-dose.

Excretion and Mass Balance in Urine and Feces. Approximately 77% of total ^{14}C was recovered in feces, and 12% was excreted in urine through the last collection interval (Table 1). Most of the administered radioactivity was recovered in the first 240 hours postdose (>87%). Quantifiable levels of radioactivity were found in feces through 552 hours postdose (the last collection interval) and in urine through 528 hours postdose. The overall mean recovery of radioactivity in feces and urine samples was 88.96% over the 552-hour study, with recovery in individual subjects ranging from 81.00% to 91.83%.

The maximum mean concentrations of [^{14}C]-naronapride-derived radioactivity were observed in samples collected from 24 to 48 hours postdose for feces (138,000 ng-Eq/g) and 0 to 2 hours postdose for urine (36,300 ng-Eq/g).

Metabolic Profiling. The extraction recovery of radioactivity for plasma samples from one subject was 91.8% and 102.8% for 1 hr and 4 hr samples, respectively. The extraction recovery of radioactivity for fecal homogenate samples from a representative subject was 102.5% and 86.3% for 24 hr and 72 hr samples, respectively. The HPLC column recovery was determined to be 101.6% using a urine sample. No correction factors were applied to the plasma and fecal concentrations to account for the recovery.

The metabolic pathways of naronapride are shown schematically in Figure 3. Seven metabolites (ATI-7400, ATI-7500, ATI-7500 glucuronide, ATI-7100, M4, M9, and M11) were observed in the radiochromatograms of human plasma, urine, and feces and were identified using HPLC/tandem mass spectrometry. Metabolites quinuclidinol and M6 were identified as non-radiolabeled products. M9, a hydroxylation metabolite with the hydroxyl group on the piperidine ring, was observed only in urine in 2 of the 8 subjects and comprised less than 0.06% of the naronapride dose. M11, a glycoside of naronapride, was identified only in fecal samples, and the level was too low to be quantitated. Representative HPLC radiochromatograms for metabolites in plasma, urine and feces are shown in Figure 4.

The fragmentation pattern of naronapride standard was studied to facilitate the interpretation of the mass spectra of its metabolites. The mass spectrum of naronapride (Supplemental Figure 5) showed a protonated molecular ion at *m/z* 537; an isotope peak at *m/z* 539 was also observed due to the presence of a chlorine atom in the molecule. The product ion spectrum of *m/z* 537 (Supplemental Figure 6) showed a peak at *m/z* 505 which was formed by a loss of methanol, probably on the piperidine ring. The base peak *m/z* 305 on the product ion spectrum was formed from *m/z* 505 by the loss of the amide moiety on the piperidine ring. Fragments at *m/z* 184 and *m/z* 380 are shown in Figure 6 (Supplemental).

Metabolite Identification

Naronapride. The mass spectrum of the peak at about 8.5 minutes (Supplemental Figure 7, top panel) showed molecular ions at *m/z* 537 and 539. The product ion spectrum of *m/z* 537 (Supplemental Figure 7, bottom panel) was the same as that of naronapride standard.

Metabolite ATI-7500 (M2). The protonated molecular ion of metabolite ATI-7500 was m/z 428, and an isotope peak at *m/z* 430 indicated that one chlorine was present in the molecule. This metabolite was proposed as a product formed from hydrolysis of the ester bond, and its product ion spectrum (Supplemental Figure 8) matched that of the standard ATI-7500. The peak at *m/z* 396 was formed by a loss of methanol from the piperidine ring. The base peak at *m/z* 196 was

formed from *m/z* 396 by the loss of the amide moiety from the piperidine ring. Peak *m/z* 184 was formed from *m/z* 428 by the cleavage of the amide bond. The product ion spectrum was the same as that of ATI-7500 standard.

Metabolite ATI-7400 (M1). The protonated molecular ion of metabolite ATI-7400 was *m/z* 400, and an isotope peak at *m/z* 402 indicated that one chlorine was present in the molecule. This metabolite was proposed as a product formed from metabolite ATI-7500 by β-oxidation, and its product ion spectrum (Supplemental Figure 9) matched that of the standard ATI-7400. The peak at *m/z* 368 was formed by a loss of methanol from the piperidine ring. The peak at *m/z* 68 was formed from *m/z* 368 by the loss of the amide moiety from the piperidine ring. Peak *m/z* 184 was formed from *m/z* 400 by the cleavage of the amide bond. The product ion spectrum was the same as that of ATI-7400 standard.

Metabolite ATI-7100 (M3). The protonated molecular ion of metabolite ATI-7100 was *m/z* 372, and an isotope peak at *m/z* 374 indicated that one chlorine was present in the molecule. Sodium adduct ions at *m/z* 394 and 396 were also observed on the mass spectrum. This metabolite was proposed as a product formed from metabolite ATI-7400 by β-oxidation, and its product ion spectrum (Supplemental Figure 10) matched that of the standard ATI-7100. The peak at *m/z* 340 was formed by a loss of methanol from the piperidine ring. The peak at *m/z* 140 was formed from *m/z* 340 by the loss of the amide moiety from the piperidine ring. Peak *m/z* 184 was formed from *m/z* 372 by the cleavage of the amide bond. The product ion spectrum was the same as that of ATI-7100 standard.

Metabolite M4. The protonated molecular ion of metabolite M4 was *m/z* 314, and an isotope peak at *m/z* 316 indicated that one chlorine was present in the molecule. Fragment peaks at *m/z* 184 and 186 were also observed. The product ion spectrum of *m/z* 314 (Supplemental Figure 11) showed a base peak at *m/z* 184 and a peak at *m/z* 282. The peak at *m/z* 282 was formed from *m/z* 314 by a loss of methanol from the piperidine ring. Peak *m/z* 184 was formed from

m/z 314 by the cleavage of the amide bond. The metabolite M4 was proposed to be a product formed from naronapride by N-dealkylation.

Metabolite M9. The protonated molecular ion of metabolite M9 was *m/z* 553, and an isotope peak at *m/z* 555 indicated that one chlorine was present in the molecule. The molecular ion of M9 was 16 Da more than that of naronapride and was therefore an oxidation product of naronapride. The product ion spectrum of *m/z* 553 (Supplemental Figure 12) showed a peak at *m/z* 521 that was formed by a loss of methanol on the piperidine ring. The peak at *m/z* 321 on the product ion spectrum was formed from *m/z* 521 by the loss of the amide moiety on the piperidine ring. Loss of H_2O from *m/z* 321 formed fragment *m/z* 303. Based on the fragmentation of *m/z* 553, metabolite M9 was proposed to be a hydroxylation metabolite of naronapride with the hydroxyl group on the piperidine ring.

Metabolite M12. The protonated molecular ion of metabolite M12 was *m/z* 604, and an isotope peak at *m/z* 606 indicated that one chlorine was present in the molecule. The molecular ion of M12 was 176 Da more than that of ATI-7500 (*m/z* 428) and was therefore a glucuronide conjugate of ATI-7500. The product ion spectrum of *m/z* 604 (Supplemental Figure 13) showed a peak at *m/z* 428 that was formed by a loss of glucuronide. The base peak at *m/z* 360 retained the glucuronide moiety and was formed by the cleavage of amide bond. The peak at *m/z* 572 was formed by the loss of methanol. Based on the fragmentation of *m/z* 604, metabolite M12 was proposed as N-glucuronide of ATI-7500.

Metabolite M11. The protonated molecular ion of metabolite M11 was *m/z* 699, and an isotope peak at *m/z* 701 indicated that one chlorine was present in the molecule. The molecular ion of M11 was 162 Da more than that of naronapride and was therefore a glycoside of naronapride. The product ion spectrum of *m/z* 699 (Figure 14) showed peak at *m/z* 537 which was formed by loss of a hexose (glucose or galactose) moiety. The base peak at *m/z* 346 retained the sugar moiety and was formed by the cleavage of amide bond. Fragments at *m/z* 681 and 663 were formed by loss of H_2O. A fragment at *m/z* 579 is shown in Figure 14 (Supplemental). Based on

the fragmentation of *m/z* 699, metabolite M11 was proposed as a glycoside of naronapride (glucose or galactose).

Metabolites M5 and M6. Because metabolite ATI-7500 was formed from the hydrolysis of the ester bond of naronapride, its corresponding non-radiolabeled part, 3-quinuclidinol (M5), was expected to be formed. The extracted ion chromatogram of *m/z* 128 (protonated molecular ion of M5) showed a peak at 3.95 min (Supplemental Figure 15, top panel). The product ion spectrum of *m/z* 128 from human urine (Supplemental Figure 15, bottom panel) was the same as the standard of 3-quinuclidinol (Sigma-Aldrich, St. Louis, MO). Another non-radiolabeled metabolite M6 (*m/z* 256), formed from N-dealkylation at the piperidine nitrogen of naronapride, was also expected and found. The extracted ion chromatogram of *m/z* 256 (molecular ion of M6) showed a peak at 8.16 min (Supplemental Figure 16, top panel). The product ion spectrum of *m/z* 256 from human urine (Supplemental Figure 16, bottom panel) showed a base peak at *m/z* 128 which corresponded to 3-quinuclidinol, and other peaks at *m/z* 110, 194, and 238.

Metabolites Observed in Plasma. Naronapride underwent a rapid esterase hydrolysis to ATI-7500 with the stoichiometric loss of quinuclidinol. This hydrolytic step is known to happen in human plasma *in vitro* (Aryx Therapeutics, unpublished results) and also in human liver microsomes (*vide infra)*. ATI-7500 was then either glucuronidated to phenyl N-glucuronide (M12), or its hexanoic acid side chain underwent two-carbon cleavage to form ATI-7400. The butanoic acid side chain of ATI-7400 underwent a further two-carbon cleavage to form ATI-7100. All of these products were major metabolites of naronapride as indicated by their higher exposure in plasma compared to parent drug and were likely formed in metabolic organs, e.g.., liver and intestine. Due to the fact that ATI-7500 glucuronide co-eluted with parent drug during metabolite profiling (Supplemental Figure 5), quantitation of this metabolite was not feasible using HPLC coupled with radiomatic detection. Even though ATI-7500 glucuronide appeared to comprise a major portion of the combined peak with naronapride in plasma, it was excreted only in urine and comprised no more than 0.36% of the dose. A very minor amount of

naronapride was found to undergo an N-dealkylation to form M4 with a concomitant loss of the M6 metabolite. Metabolite M4 was below the quantification limit (defined as a 3 to 1 signal to noise on the radiochromatogram) in 4 of the 8 subjects. M6 could not be quantitated due to its lack of radioactivity.

Excretion of Naronapride and its Major Metabolites. Mean percentages of the naronapride dose recovered as urine and fecal radioactivity, naronapride, and its major metabolites are given in Table 1. Approximately one third of the ^{14}C dose was recovered as parent drug, mainly in feces. Overall, ATI-7500, ATI-7400 and ATI-7100 accounted for 36.56%, 16.28% and 1.58%, respectively, of the dose. Quinuclidinol would be presumed to be approximately equal to the sum of all the metabolites that had a loss of the quinuclidinol moiety (~ 54% of dose).

Metabolite ATI-7400 was the major radioactive component in the urine of all subjects. The cumulative urinary recovery for ATI-7400 ranged from 3.84% for subject 4 to 12.75% for subject 5. The cumulative urinary recovery for ATI-7500 ranged from 0.20% for subject 4 to 1.86% for subject 5. The cumulative urinary recovery for naronapride and M12 together ranged from 0.11% for subject 4 to 1.03% for subject 5. The cumulative urinary recovery for all radioactive components ranged from 6.11% for subject 4 to 21.78% for subject 5.

Naronapride and metabolite ATI-7500 were the major radioactive components in the feces of all subjects. The cumulative recovery in feces for naronapride ranged from 4.40% for subject 7 to 63.37% for subject 1. The cumulative recovery in feces for ATI-7500 ranged from 5.84% for subject 1 to 66.61% for subject 3. The cumulative recovery in feces for all radioactive components ranged from 68.92 % for subject 5 to 82.82% for subject 4.

***In Vitro* Metabolism.** The half-life of naronapride (2 µM) exceeded 90 minutes in human liver microsomes (1 mg/mL), and rates of degradation were not dependent on the presence of the NADPH-generating system. Naronapride was hydrolyzed to yield a single acid metabolite, ATI-7500, and the rate of ATI-7500 formation was stoichiometrically related to the rate of naronapride loss. A very small amount of a hydroxylated naronapride metabolite was detected

but could not be quantified; its formation was dependent on time and the NADPH-generating system. The site of oxidation on naronapride was identified by LC/MS/MS product ion scan analysis using the fragmentation patterns observed for the parent molecule and its oxidation metabolite. Based on these patterns, the piperidine ring and/or the quinuclidine ring were identified as possible hydroxylation sites.

When incubated with human hepatocytes, naronapride (10 µM) was reduced by half after 194 minutes. The metabolite, ATI-7500, was monitored and its formation was observed to lack the clear stoichiometric relationship with the loss of naronapride that was observed with the microsomal incubations, and small amounts of ATI-7400 resulting from the cleavage of two carbon atoms from the hexanoic acid side chain of ATI-7500 were detected. Approximately 77% of naronapride remained at the end of 6 hr; ATI-7400 comprised 1 to 3% of naronparide metabolized. The formation of ATI-7500 and ATI-7400 together accounted for 41.1% of the metabolism of naronapride (33.6% and 7.5%, respectively). The formation of an oxidative (M+16) metabolite of naronapride was detected in hepatocyte samples. The site of oxidation was identified using the fragmentation pattern observed for naronapride and its oxidation metabolite by product ion scan analysis. Based on the fragmentation patterns, there were two possible sites of oxidation: on the piperidine ring or the quinuclidine ring. The potential for oxidation on the quinuclidine ring was tested by incubating naronapride (10 µM) in human hepatocytes. After a 5 or 6 hr incubation, the samples were split. One set of samples was quenched immediately, and the other set was incubated at 37°C with equine butyrylcholinesterase (BuChE) for 20 min then quenched. The amount of oxidative metabolite remaining when the samples were further incubated with BuChE was significantly less than in the samples that were not exposed to BuChE. In addition, there was a concomitant increase in the amount of ATI-7500 and hydroxy quinuclidinol formed. These results suggest that oxidation of naronapride could take place at a site on the quinuclidine ring of the parent molecule prior to hydrolysis to ATI-7500 and hydroxy quinuclidinol. Naronapride, ATI-7500, ATI-7400, and

ATI-7100 were stable in KH buffer during the period of incubation. This result indicated that the degradation of the test articles observed in the hepatocyte suspensions was due to enzyme-mediated metabolism and not to chemical instability. Diclofenac (control standard) was metabolized rapidly. The amount of diclofenac remaining at the end of 6 hr incubation was approximately 9%. The Phase I metabolite (4-hydroxy diclofenac) and Phase II metabolites (diclofenac glucuronide and hydroxy diclofenac glucuronide) were formed and indicated that Phase I and Phase II enzymes were active in the hepatocyte system.

A significant portion of naronapride metabolized in hepatocytes (>50%) was not accounted for by metabolites for which chemical standards were available. A more detailed description of these *in vitro* observations will be published elsewhere.

***In Vitro* Plasma Protein Binding.** Plasma protein binding of naronapride and its principal metabolites, ATI-7500, ATI-7400, and ATI-7100, are given in Table 2. Binding of [^{14}C]-naronapride to human plasma protein was approximately 30 to 41% and was independent of plasma drug concentration throughout the range tested (0.045 to 450 µM). Protein binding of the metabolite, [^{14}C]-ATI-7500 was lower than that of the parent drug and tended to decrease (from 40% to 25% over the [^{14}C]-ATI-7500 concentration range of 0.064 to 640 µM. Plasma protein binding of ATI-7400 and ATI-7100 were approximately 44% and 65%, respectively, across the concentration range tested (2.5 to 10 µM).

Plasma Pharmacokinetics. Plasma levels of ATI-7500, ATI-7400 and ATI-7100 determined using HPLC coupled with radiomatic detection and by LC/MS/MS were generally consistent with each other. Mean plasma concentration profiles for naronapride and its major metabolites based on LC/MS/MS measurements are shown in Figure 2.

Pharmacokinetic parameters for naronapride and its major metabolites (based on LC/MS/MS assay results) are given in Table 3. Highest concentrations (C_{max}) of naronapride were achieved approximately 45 minutes postdose with the mean value of 13.34 ng-Eq/mL. The terminal elimination half-life ($t_{1/2}$) of naronapride averaged 5.36 hr. Naronapride was

extensively metabolized, and the exposure, as measured by AUC, for quinuclidinol, ATI-7500, ATI-7400 and ATI-7100 was approximately 72-, 17-, 8-, and 2.6-fold higher than that of parent drug. ATI-7500 and quinuclidinol reached peak plasma levels within 1 hour after dose, indicating rapid esterase hydrolysis of naronapride. Peak concentrations for ATI-7400 and ATI-7100 were both reached within 1.7 hour postdose. Cumulatively, naronapride, ATI-7500, ATI-7400 and ATI-7100 accounted for approximately 72% of the radioactivity in plasma, using AUC measurement. ATI-7500 glucuronide (M12), which was not quantitated by LC/MS/MS, may have contributed to some extent to the unaccounted radioactivity in plasma. The plasma concentration profiles for all major metabolites determined by LC/MS/MS were largely parallel to each other, and their average terminal half-lives ($t_{1/2,z}$) ranged between 17.69 and 33.03 hours.

DISCUSSION

This study determined the absorption and disposition of the selective 5-HT_4 receptor partial agonist, naronapride, in healthy male volunteers given a single oral 120-mg dose of [^{14}C]-naronapride (200 µCi). Naronapride was rapidly absorbed with a t_{max} of approximately 45 min. The absolute oral bioavailability of naronapride is not known, however the small amount of the dose recovered in the urine (12%), the relatively low amounts of naronapride in plasma, and the large amounts of unchanged drug present in the feces (32%), are consistent with it being low. The oral bioavailability of naronapride in rats and dogs is approximately 25% (ARYx Therapeutics, unpublished results) and supports this speculation. The presence of naronapride in feces has important therapeutic implications, as accumulating evidence indicates that the enterokinetic actions of 5-HT_4 agonists are mediated by the facilitation of synaptic transmission in the gut myenteric plexus by blood-borne drug and by local interactions with targets in the intestinal mucosal epithelium (Grider et al.; 1998; Jin et al., 1999; Balemba & Mawe, 2009). Accordingly, the current findings suggest the prokinetic actions of naronapride could result from both its systemic uptake and local interactions with the colonic epithelium.

At the t_{max}, [^{14}C]-naronapride accounted for approximately 9% of the radioactivity in plasma reflecting its rapid hydrolysis and subsequent putative β-oxidation to ATI-7500, ATI-7400, and ATI-7100. The apparent plasma terminal half-life of naronapride was lower in this investigation (5.36 hr) than $t_{1/2}$ values obtained in another pharmacokinetics study (120 mg oral dose; mean $t_{1/2}$ = 21 hr [range = 6-38 hr]; ARYx Therapeutics, unpublished findings) where the naronapride LLOQ was 0.05 ng/mL (versus 0.1 ng/mL in the present study) and plasma samples were collected more frequently to more closely define the terminal phase of the naronapride concentration versus time curve. These findings, when considered with evidence that intraluminal naronapride can act locally to increase gut motility (approximately 32% of the oral dose was excreted unchanged in feces), are consistent with twice-a-day dosing and suggest that once-a-day dosing may also be effective.

Naronapride was specifically designed to undergo metabolism by tissue and circulating esterases in order to minimize cytochrome P450-mediated drug-drug interactions. Results of this study confirmed that, as designed, naronapride is principally subject to rapid hydrolysis. In all, seven major naronapride metabolites were identified in plasma (Figure 3): ATI-7500, a hydrolysis product is formed by cleavage of the ester bond; ATI-7400, an oxidation product of ATI-7500; ATI-7100, an oxidation metabolite of ATI-7400; a glucuronide of ATI-7500 (M12); an N-dealkylation product of naronapride (M4); a hydroxylation product of naronapride (M9); and a glycoside of naronapride (M11). The detection of M11 in feces was unusual given that the mass spectrometric interpretation indicated that it was a glycoside conjugate of naronapride. The molecular ion of M11 was 162 Da more than that of naronapride and the product ion spectrum of m/z 699 showed peak at m/z 537, which was formed by loss of hexose (glucose or galactose) moiety. In addition, N-glucosides have been noted in the literature as conjugates present in urine and bile from other mammalian species and this metabolite represented only a very minor pathway for elimination (Tang, 1990; Tang et al., 2003; Nakazawa et al., 2006). Two metabolites without ^{14}C label were 3-quinuclidinol, an ester hydrolysis product of naronapride

and an N-dealkylation product of naronapride with dealkylation at piperidine nitrogen (M6). ATI-7500, ATI-7400, and ATI-7100 together accounted for most of the radioactivity in plasma (70%). O-dealkylation could lead to the loss of label, but because most of the dose was recovered in the plasma, urine, and feces, the amount of metabolite formed via this pathway must be negligible. *In vitro* binding and cell-based functional assays showed that ATI-7500, ATI-7400 and ATI-7100 are weak partial agonists of human 5-$HT_{4(b)}$ receptor and have no meaningful affinities for dopamine D_2 receptors. Like naronapride, ATI-7500, ATI-7400, ATI-7100 have negligible affinity for cardiac I_{Kr} channels and were essentially devoid of electrophysiological effects in guinea pig myocardium. Broad receptor profiling and affinity data have been collected for the ATI-7500 metabolite only. In wide-spectrum competitive radioligand binding assays, ATI-7500 had no relevant affinity for a diverse array of more than 64 molecular targets including receptors, ion channels, and transporters.

Naronapride hydrolysis to ATI-7500 by esterases appears to be a primary route of naronapride metabolism in hepatic microsomes. The rate of naronapride degradation by human liver microsomes was not dependent on the presence of NADPH indicating that naronapride loss was primarily by esterase-mediated hydrolysis and not oxidative metabolism in this subcellular fraction. A small, though not quantified, amount of a hydroxylated metabolite was detected after incubation of naronapride with microsomes and its formation was time dependent and required the addition of the NADPH-generating system. The formation of this metabolite could be due to CYP450-mediated oxidative ester hydrolysis of naronapride, however further work would be required to confirm this hypothesis. Thus, although some CYP450 involvement in naronapride metabolism was found in human liver microsomes, collectively these data suggest that naronapride is a poor substrate for CYP450.

In contrast to the results of the metabolism of naronapride with human liver microsomal preparations, incubation with human hepatocytes led to the formation of metabolites other than ATI-7500 (e.g., ATI-7500 formation accounted for only 34% of naronapride metabolism). One of

these, ATI-7400 (an oxidation product resulting from a two carbon cleavage of the hexanoic acid side chain of ATI-7500) was possibly a product of β-oxidation, a process that occurs in mitochondria and peroxisomes and is normally associated with fatty acid metabolism (Suga, 2003). Liver microsomes are a post-mitochondrial fraction, and this probably accounts for the lack of ATI-7400 or ATI-7100 formed in incubations using this preparation.

The primary route of elimination of recovered radioactivity was via fecal excretion (77%), and naronapride was mainly eliminated through hydrolysis reactions and excretion of unchanged drug. Hydrolytic cleavage of the quinuclidinol moiety accounted for the elimination of 36.56% of the dose (0.93% in urine and 35.63% in feces). ATI-7500 was subject to sequential 2-carbon cleavage of its aliphatic acid side chain, and peak concentrations for ATI-7400 and ATI-7100 were reached within one hour of the naronapride t_{max}, indicating that the process was fairly rapid. Quinuclidinol plasma concentrations reached peak levels within 1 hour after dosing, and the overall AUC was approximately 4-times that of ATI-7500, ATI-7400, and ATI-7100 combined. Oxidation of the quinuclidine moiety was detected in hepatocytes and findings suggested this occurred prior to naronapride hydrolysis to ATI-7500. In another study, quinuclidinol, at concentrations to 10 µM, was stable over a 90 minute incubation period in *in vitro* incubations with mouse, rat, and human liver S9 fractions at 37°C, i.e., neither hydroxylated derivatives of quinuclidinol nor other potential biotransformation products were detected (Procter and Gamble, unpublished findings).

The qualitative metabolic profile for naronapride is similar between mice, rats, dogs, and humans. For example, after administration of a single 500 mg/kg oral dose of [^{14}C]-naronapride to male mice, the plasma drug related compounds, listed in order of AUC exposure to the major human metabolites relative to naronapride [with approximate X-fold ratios] were: quinuclidinol [~8.8], ATI-7500 [~4.6], ATI-7400, [~3-5], naronapride [1] and ATI-7100 [0.4]. Exposures after a single oral dose of 300 mg/kg [^{14}C]-naronapride in male rats, listed in order of AUC exposure

relative to naronapride [with approximate X-fold ratios] were: quinuclidinol [~3.5], ATI-7500 [~1.3], ATI-7505 [1], ATI-7400 [~0.3] and ATI-7100 [~0.02].

In summary, [^{14}C]-naronapride was rapidly absorbed in fasting healthy human subjects after a single oral dose of 120 mg. Plasma protein binding was low (~30 to 40%), and the blood-to-plasma radioactivity concentration ratios (ranging from 0.570 to 0.683 through 4 hours post-dose) indicated minimal partitioning of ^{14}C into red blood cells. Four major circulating naronapride metabolites were identified in plasma, i.e. quinuclidinol, ATI-7500, ATI-7400, and ATI-7100. Plasma naronapride levels were low relative to quinuclidinol, ATI-7500, and ATI-7400. Naronapride underwent extensive systemic metabolism and the apparent terminal plasma half-life of naronapride was approximately 5 hr. Elimination of [^{14}C]-naronapride mainly involved fecal excretion of unabsorbed drug, a naronapride hydrolysis product (ATI-7500) and two additional products (ATI-7400 and ATI-7500). None of these metabolic pathways appear to be CYP450 mediated. Naronapride is currently in development for the treatment of chronic idiopathic constipation.

ACKNOWLEDGMENTS

The authors thank the staffs of the Experimental Medicine Group and the Analytical Sciences Department of Procter and Gamble Pharmaceuticals (Mason, OH), Convince Clinical Research Unit (Madison, WI), Convince Laboratories (Madison, WI), and QPS (Newark, DE) and Study Directors/Principal Investigators S. Flash, M.D., JP Mainwaring, Ph.D., C.S. Oakley, B.A., and R. Wang, Ph.D. for the conduct of this study.

AUTHORSHIP CONTRIBUTION

Participated in research design: R. Coleman, A. Davies, P. Kumaraswamy, L. Lightning, S. Rao

Conducted experiments: R. Coleman, A. Davies, P. Kumaraswamy, S. Rao

Performed data analysis: S. Bowersox, R. Coleman, A. Davies, P. Kumaraswamy, L. Lightning, S. Rao

Wrote or contributed to the writing of the manuscript: S. Bowersox, R. Coleman, A. Davies, P. Druzgala, D. Ellis, P. Kumaraswamy, L. Lightning, M. Palme, S. Rao

REFERENCES

Balemba OB, Mawe GM (2009) Effects of ATI-7505 on propulsive motility and fast synaptic potentials in the guinea pig colon. *Neurogastroenterol Motil* **21**:86.

Boudinot FD, Jusko WJ (1984) Fluid shifts and other factors affecting plasma protein binding of prednisolone by equilibrium dialysis. *J Pharm Sci* **73**:774-80.

Camilleri M (2001) Review article: tegaserod. *Aliment Pharmacol Ther* **15**:277-89.

Camilleri M, Vazquez-Roque MI, Burton D, Ford T, McKinzie S, Zinsmeister AR, Druzgala P (2007) Pharmacodynamic effects of a novel prokinetic 5-HT receptor agonist, ATI-7505, in humans. *Neurogastroenterol Motil* **19**:30-8.

Camilleri M, Andresen V (2009) Current and novel therapeutic options for irritable bowel syndrome management. *Digestive and Liver Disease* **41**:854-62.

Camilleri M, Bharucha AE (2010) Behavioral and new pharmacological treatments for constipation: getting the balance right. *Gut* **59**:1288-96.

USFDA Center for Drug Evaluation and Research (2002) Drug Approval Package: Zelnorm (Tegaserod Maleate); Application No.: 21-200.

Grider JR, Foxx-Orenstein AE, Jin JG (1998) 5-Hydroxytryptamine4 receptor agonists initiate the peristaltic reflex in human, rat, and guinea pig intestine. *Gastroenterology* **115**(2):370-80.

Jin JG, Foxx-Orenstein AE, Grider JR (1999) Propulsion in guinea pig colon induced by 5-hydroxytryptamine (HT) via 5-HT_4 and 5-HT_3 receptors. *J Pharmacol Exp Ther* **288**(1):93-7.

Manabe N, Wong BS, Camilleri M (2010) New-generation 5-HT_4 receptor agonists: potential for treatment of gastrointestinal motility disorders. *Expert Opin Investig Drugs* **19**(6):765-75.

Milner PG, Canafax DM, Palme M, Morganroth J (2010) Results of a thorough QT Study (ICH E14) testing a novel gastrointestinal prokinetic, ATI-7505, show no ECG effects at therapeutic and supra-therapeutic doses. *Gastroenterology* **138** (5, suppl 1):S164-S165.

Mohammad S, Zhou Z, Gong Q, January CT (1997) Blockage of the HERG human cardiac K+ channel by the gastrointestinal prokinetic agent cisapride. *Am J Physiol* **273**(5 Pt 2):H2534-8.

Nakazawa T, Miyata K, Omura K, Iwanaga T, Nagata O (2006) Metabolic profile of FYX-051 (4-(5-pyridin-4-yl-1H-[1,2,4]triazol-3-yl)pyridine-2-carbonitrile) in the rat, dog, monkey, and human: Identification of N-glucuronides and N-glucosides. *Drug Metab Dispos* **34**(11):1880-1886

Palme M, Milner PG, Bandman O, Ziola M, Canafax, DM (2010) A novel gastrointestinal prokinetic, ATI-7505, increased spontaneous bowel movements (SBMs) in a phase II, randomized, placebo-controlled study of patients with chronic idiopathic constipation (CIC). *Gastroenterology* **138**(5, suppl 1):S128-S129.

Pau D, Workman AJ, Kane KA, Rankin AC (2005) Electrophysiological effects of prucalopride, a novel enterokinetic agent, on isolated atrial myocytes from patients treated with beta-adrenoceptor antagonists. *J Pharmacol Exp Therap* **313**:146-53.

Suffredini S, Cerbai E, Giunti G, El Mouelhi M, Pfannkuche HJ, Mugelli A (2010) Electrophysiological characterization of isolated human atrial myocytes exposed to tegaserod. *Basic Clin Pharmacol Toxicol* **106**(5) 416-21.

Suga T (2003) Drug metabolism in peroxisomes: involvement of peroxisomal beta-oxidation system in the oxidative chain-shortening of xenobiotic acyl compounds. *Drug Metab Pharmacokinet* **18**(3):155-62.

Tang B-K (1990) Drug glucosidation. *Pharmac Ther* **46**:53-56.

Tang C, Hochman JH, Ma B, Subramanian R, Vyas KP (2003) Acyl glucuronidation and glucosidation of a new and selective enthothelin ET_A receptor antagonist in human liver microsomes. *Drug Metab Dispos* **31**(1):37-45.

FOOTNOTES

The following abstracts report findings discussed in this paper: Choppin A, Palme M, Otterson M, Dennis D, Jacoby H, Druzgala P (2005) Effect of ATI-7505, a selective 5-HT_4 receptor agonist, on gastric emptying. *American College of Gastroenterology* Poster abstract #750308; Nie Y, Palme M, Dennis D, Druzgala P, Choppin A, Chen J, Sarna S (2005) ATI-7505, a novel and selective 5-HT_4 receptor agonist, accelerates gastric emptying of solid meals in dogs. *American College of Gastroenterology* Poster abstract #750309; Palme M, Dennis D, Irwin I, Teichman S, Druzgala P (2004) ATI-7505 is a novel, selective 5-HT_4 receptor agonist that causes gastrointestinal prokinetic activity in dogs. *Digestive Disease Week* Poster abstract #101329; Palme M, Dennis D, Choppin A, Irwin I, Green T, Milner P, Druzgala P (2005) Cardiac safety and phase I clinical data for ATI-7505, a selective 5-HT_4 receptor agonist. *Digestive Disease Week* Poster abstract #750309.

LEGENDS FOR FIGURES

Figure 1. Structure of naronapride. The asterisk indicates the position of the ^{14}C label at the methoxy carbon on the phenyl ring.

Figure 2. Mean concentrations of radioactivity in blood and plasma following a single 120 mg (200 µCi) oral dose of [^{14}C]-naronapride to healthy male subjects. Levels of radioactivity fell below the limit of quantitation in all subjects by 6 and 12 hrs postdose in blood and plasma, respectively (upper panel). Mean plasma analyte concentration-time profiles based on LC/MS assay. ATI-7505 is naronapride. All concentrations expressed in terms of ng equivalents of naronapride (lower panel).

Figure 3. Proposed metabolic pathways of naronapride.

Figure 4. Representative radiochromatograms of naronapride in plasma taken 2 hr (upper), in urine taken 2 hrs (middle), and in fecal extracts collected approximately 48 hours (lower) after a single oral dose (120 mg/200 µCi) of [^{14}C]-naronapride was given to male subjects. The y-axis is the measured radioactivity in counts per min. The peaks at 8.5-8.9 min in the plasma and urine radiochromatograms contained metabolite M12 and naronapride which were not separated on the HPLC system. Abbreviations: ATI-7505 = naronapride; M1 = ATI-7400, M2 = ATI-7500, M3 = ATI-7100, M12 = ATI-7500 glucuronide.

Table 1. Urinary and Fecal Recovery of ^{14}C, Naronapride, and Metabolites Following Single Dose Oral Administration of 120 mg [^{14}C]-Naronapride to Healthy Subjects[a]

	A'$_e$ (%) and (%CV$_m$)		
	Urine	**Feces**	**Total**
^{14}C Radioactivity	11.96 (42.2)	77.00 (5.7)	88.96 (3.8)
Naronapride	0.45 (67.9)[a]	31.87 (60.7)	32.32 (59.8)[b]
ATI-7500	0.93 (56.1)	35.62 (62.1)	36.56 (60.3)
ATI-7400	7.77 (40.0)	8.51 (56.5)	16.28 (27.5)
ATI-7100	1.37 (66.7)	0.20 (83.8)	1.58 (65.6)

A'$_e$ (%) is the mean of the percentage of dose excreted.

%CV$_m$ is the coefficient of variation of the mean.

[a] All urine and feces was collected and analyzed

[b] Percentage of recovery of naronapride and ATI-7500 glucuronide combined. Glucuronidated ATI-7500 was not independently quantified.

Table 2. *In Vitro* Plasma Protein Binding of Naronapride and its Major Metabolites (at pH 7.4, 37°C) Across a Range of Test Article Concentrations

Compound	Concentration Range (μM)	Range of Plasma Protein Binding (% bound)
[^{14}C]-naronapride	0.045 – 450	30±3 to 41±4
[^{14}C]ATI-7500	0.064 – 640	25±3 to 40±4
ATI-7400	2.5 – 10	43±1 to 44±5
ATI-7100	2.5 – 10	65±1 to 65±2

All experiments were conducted in triplicate. Plasma protein binding data are presented as mean ± standard deviation.

Table 3. Plasma Pharmacokinetic Parameter Estimates Based on LC/MS Results.[a]

	C_{max} (ng-Eq/mL)	t_{max} (hr)	AUC_{∞} (ng-Eq·h/mL)	$t_{1/2,z}$ (hr)	Cl_o[b] (L/h/kg)	Cl_r[c] (L/h/kg)	V_z/F (L/kg)	MR[d]	$AUC_{analyte}/AUC_{14C}$
^{14}C[e]	238.63 (52.9)	0.94 (17.5)	635.17 (52.3)	2.06 (16.5)	2.80 (39.5)	CNC CNC	8.27 (41.7)	CNC CNC	CNC CNC
Naronapride	13.34 (44.2)	0.76 (34.5)	18.18 (34.0)	5.36 (52.7)	98.29 (55.8)	CNC CNC	704.20 (59.7)	CNC CNC	0.03 (42.0)
ATI-7500 (M2)	156.40 (39.8)	0.94 (17.5)	365.57 (37.6)	33.03 (14.3)	CNC CNC	0.04 (34.8)	CNC CNC	17.80 (34.4)	0.45 (11.6)
ATI-7400 (M1)	38.31 (52.3)	1.63 (31.8)	202.42 (43.1)	31.51 (33.5)	CNC CNC	0.62 (28.9)	CNC CNC	8.63 (39.9)	0.19 (17.4)
ATI-7100 (M3)	13.33 (57.1)	1.75 (26.5)	63.23 (47)	21.40 (41.1)	CNC CNC	0.34 (34.2)	CNC CNC	2.80 (39.5)	0.06 (15.4)
Quinuclidinol (M5)	274.81 (35.8)	0.94 (17.5)	2583.07 (46.8)	17.69 (67.8)	CNC CNC	CNC CNC	CNC CNC	73.84 (25.6)	CNC CNC

Values are means (% coefficient of variation of the mean); n=7-8

CNC = could not be calculated

[a] C_{max} and AUC values expressed in terms of ng equivalents of naronapride

[b] CL_o is the oral clearance, determined as the quotient of the dose divided by AUC_{∞}.

[c] CL_r is the renal clearance, determined as the quotient of the cumulative amount excreted in urine from time 0 to t_{last} divided by AUC(t_{last}).

[d] MR is the metabolite/parent ratio, based on AUC, where the AUC of the metabolite is truncated to the t_{last} of the naronapride in plasma.

[e] ^{14}C pharmacokinetic parameter estimates based on radioactivity data obtained in plasma

Fig. 1

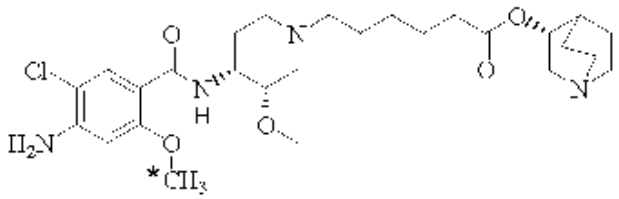

Fig. 2

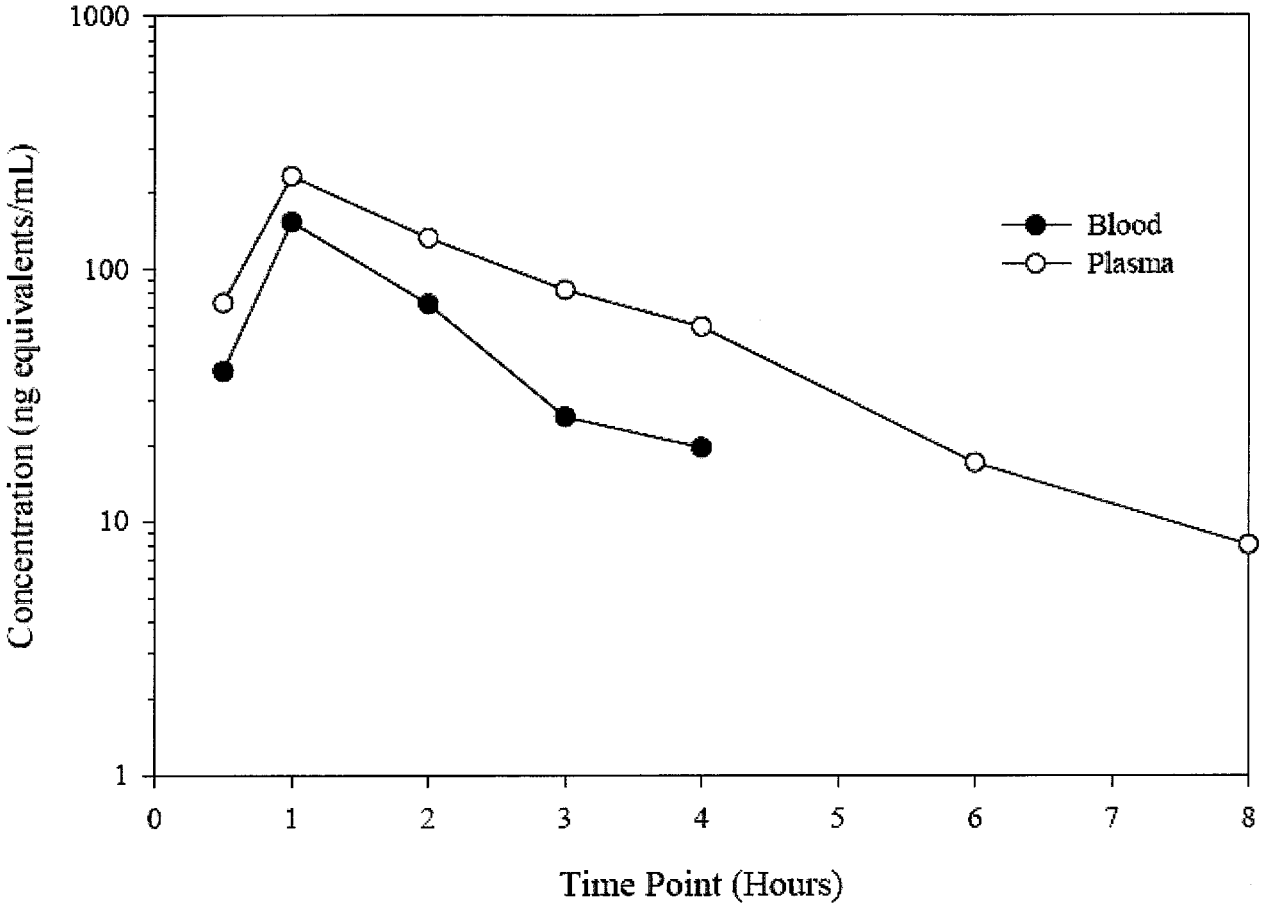
1000
100
10
1
Concentration (ng equivalents/mL)
Blood
Plasma
0
1
2
3
4
5
6
7
8
Time Point (Hours)

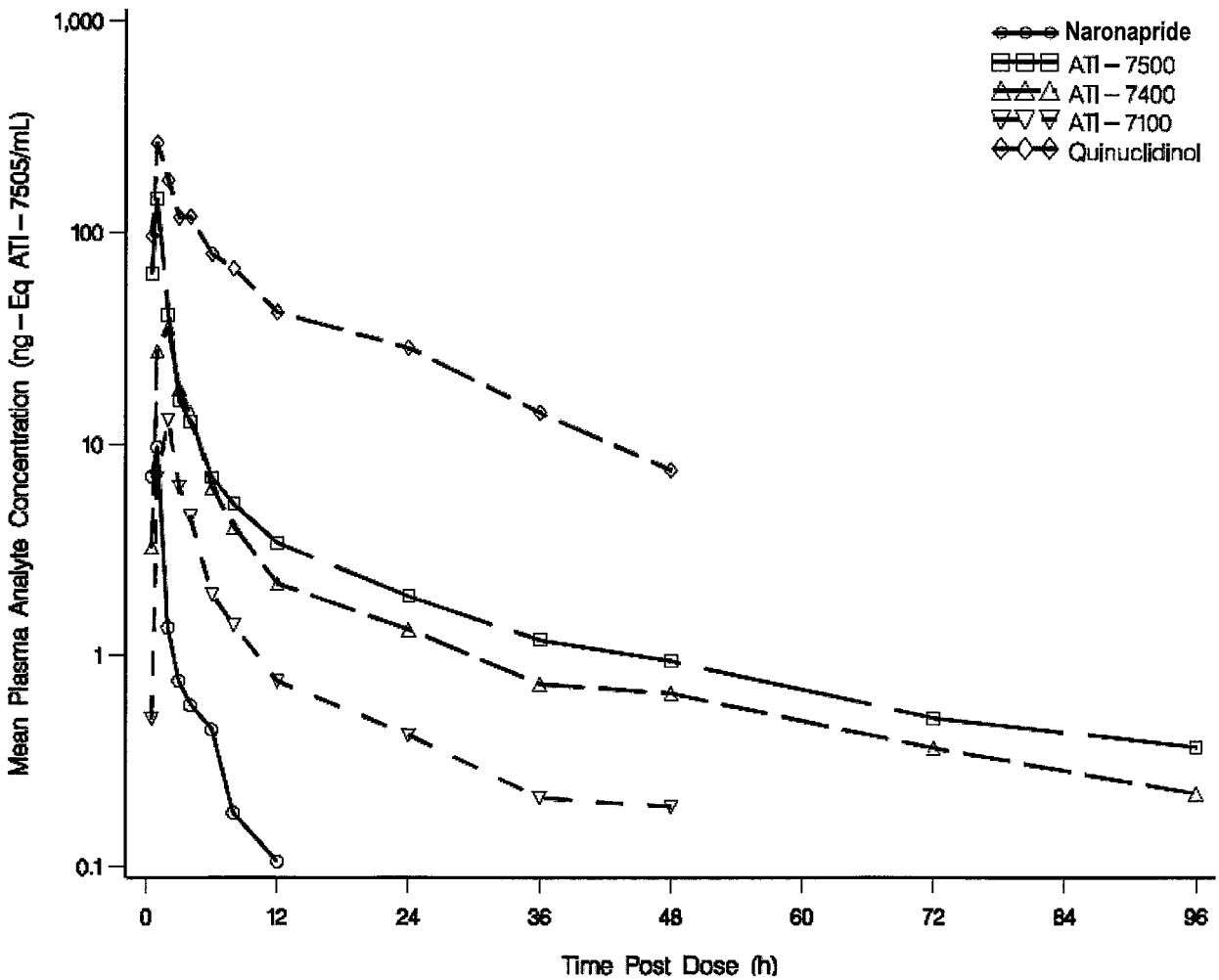
1,000
100
10
1
0.1
Mean Plasma Analyte Concentration (ng-Eq ATI-7505/mL)
Naronapride
ATI-7500
ATI-7400
ATI-7100
Quinuclidinol
0
12
24
36
48
60
72
84
96
Time Post Dose (h)

Fig. 3

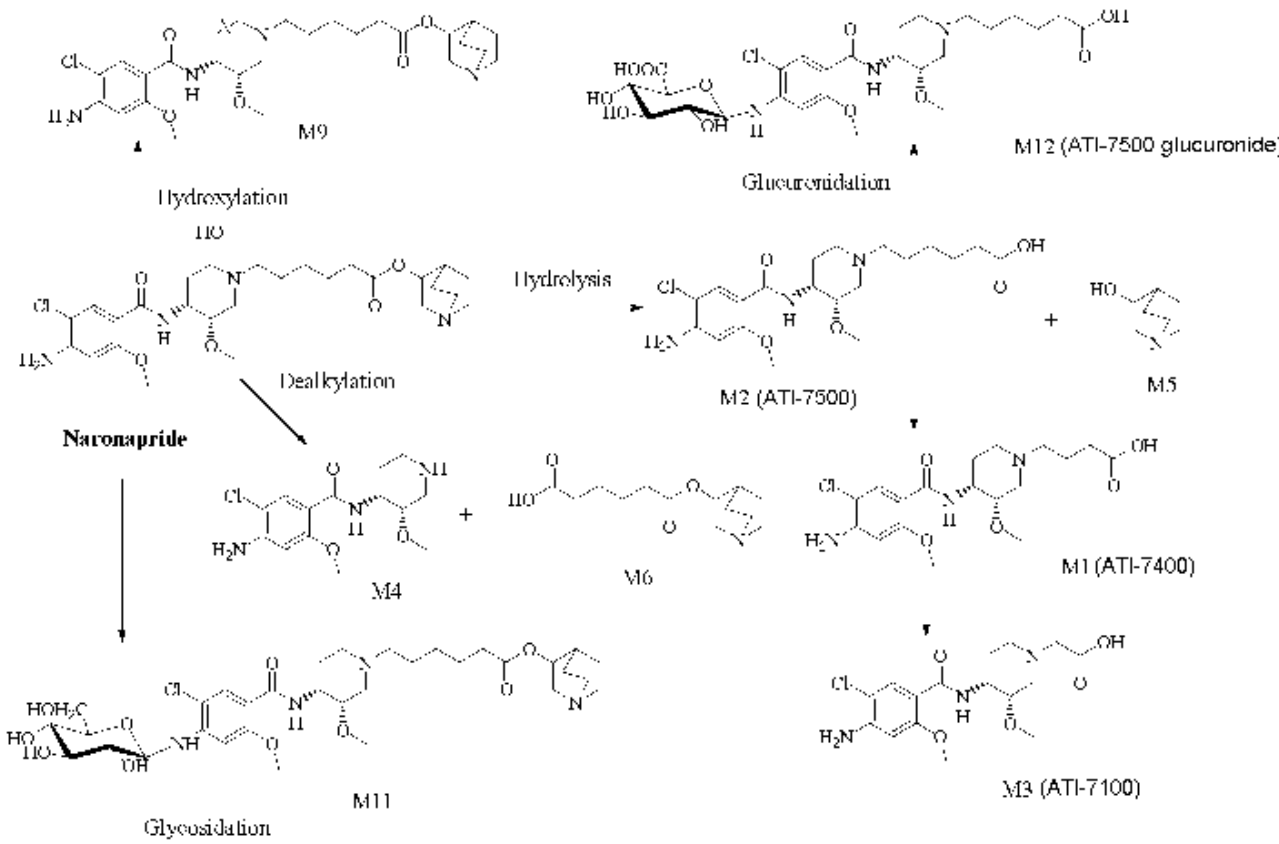
M9
Hydroxylation
M12 (ATI-7500 glucuronide)
Glucuronidation
Hydrolysis
Dealkylation
M2 (ATI-7500)
M5
Naronapride
M4
M6
M1 (ATI-7400)
M11
Glycosidation
M3 (ATI-7100)

Fig. 4

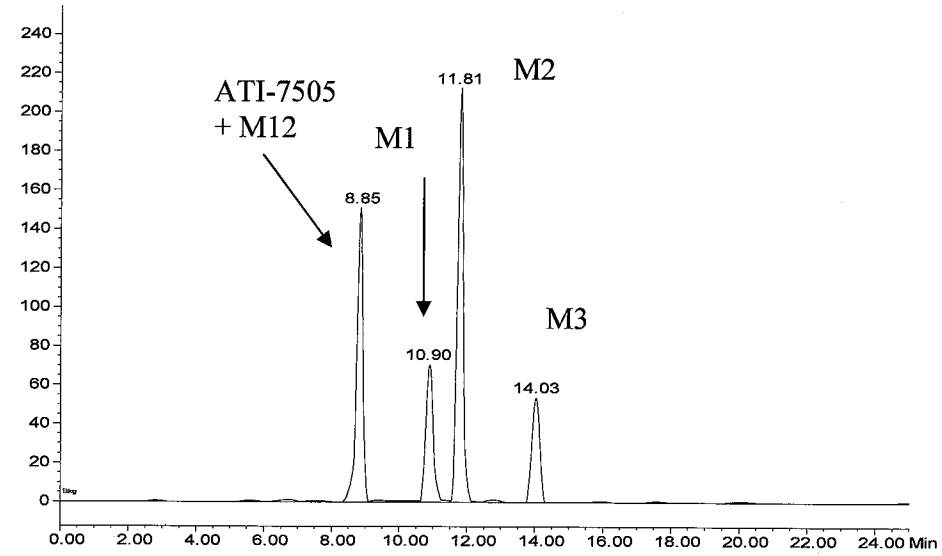
ATI-7505
+ M12
M1
M2
M3
8.85
10.90
11.81
14.03
Min

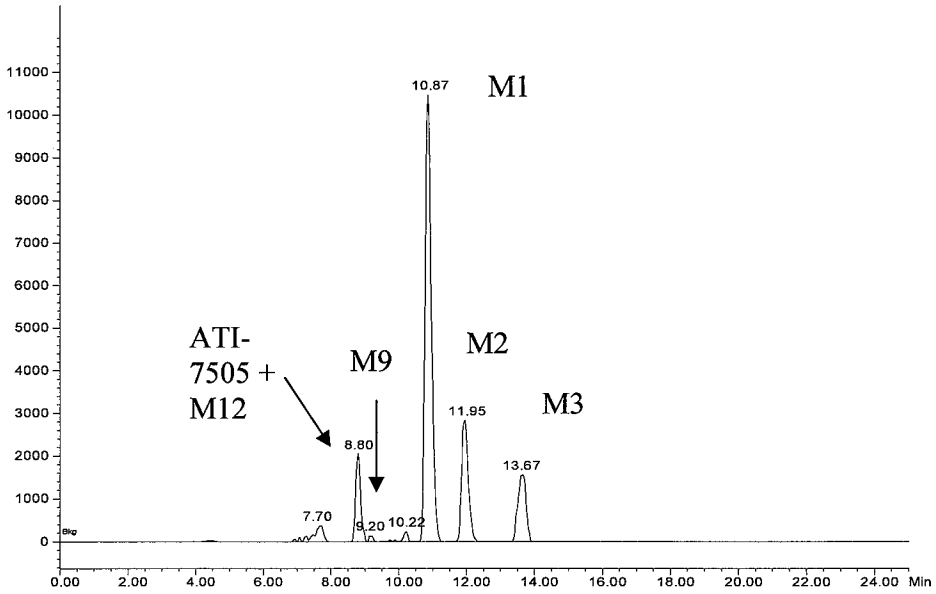
ATI-
7505 +
M12
M9
M1
M2
M3
7.70
8.80
9.20
10.22
10.87
11.95
13.67
Min

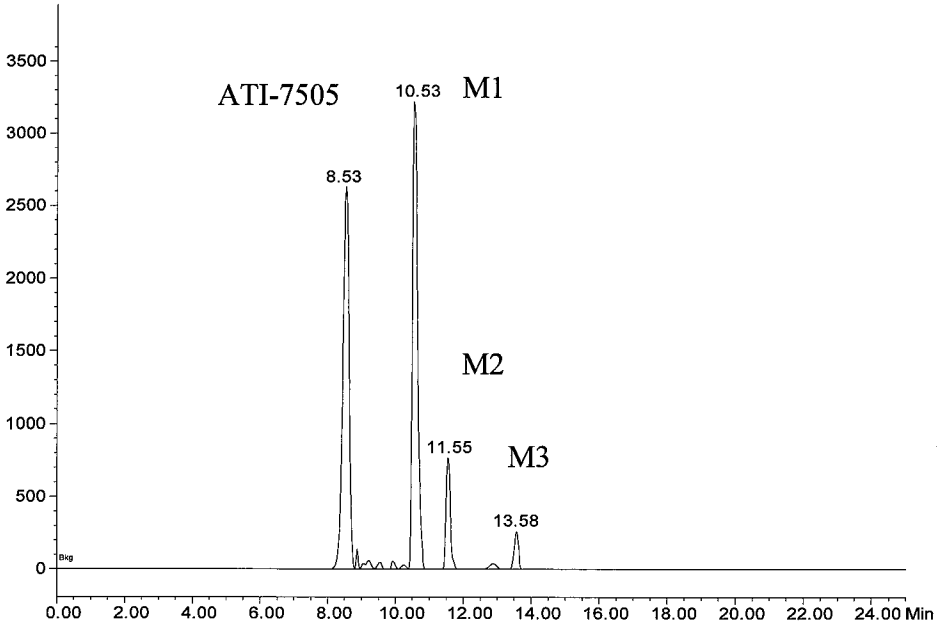
ATI-7505
M1
M2
M3
8.53
10.53
11.55
13.58
Min